Thermally Induced Optical Phase Conjugation in Solutions of C_{60} in a Variety of Organic Solvents

A. Costela,*,† I. Garcia-Moreno, and J. L. Saiz

Instituto de Química Física "Rocasolano", CSIC, Serrano 119, 28006 Madrid, Spain

Received: January 22, 1997; In Final Form: April 14, 1997[⊗]

The phase-conjugate properties of solutions of buckminsterfullerene C_{60} in a number of organic solvents have been investigated in the nanosecond time domain. Thermal grating established theory is shown to explain satisfactorily the experimental results, and evidence was found of the propagation in a nonlinear medium of acoustic waves generated by a nonuniform heating process, suggesting that a thermal mechanism is responsible for the long-lived component of the nonlinearity. Order of magnitude estimations of the thermally induced third-order susceptibility were obtained, and a correlation between effective thermalization yield and solvents' polarizability parameter $(n^2 - 1)/(2n^2 + 1)$ was found.

Introduction

Buckminsterfullerene C_{60} is a soccerball-shaped molecule consisting of 60 carbon atoms arranged in the most symmetric structure of a truncated icosahedron.[1] These molecules have a large number of conjugated double bonds providing extensive π-electron delocalization, which may lead to large nonlinear polarizabilities.[2] As a result, considerable attention has been directed toward the nonlinear optical properties of these molecules, and numerous investigations on different aspects of the nonlinearity have been carried out.[3−26] Due to the centrosymmetric structure of C_{60}, the second-order polarizability is zero, while the third-order optical polarizability is always symmetry allowed. Then, the greatest nonlinearity in these molecules should arise from the third-order susceptibility tensor $\chi^{(3)}$, which is the quantity that has attracted the interest of experimentalists.

A particularly useful technique for studying the third-order nonlinearity in these molecules is degenerate four-wave mixing (DFWM), in which two strong counterpropagating pump beams and a weak probe beam with the same frequency interact in the nonlinear medium via $\chi^{(3)}$.[27] As a result of this interaction, a new wave is generated, which is identical to the probe wave except that its spatial phase is reversed. This phase-conjugate (PC) wave will travel back along the original path of the incoming probe wave, undergoing in reverse any phase evolution that the original wave may have incurred.

There is a close analogy between the DFWM process and real-time holography.[28] The interference of two intersecting laser beams produces a spatially periodic light intensity distribution in the medium, which causes a corresponding modulation of the complex index of refraction. This modulation can be interpreted as the creation of a transient hologram by two "writing" beams. The third beam scatters off this index grating ("reads" out the transient hologram) to generate the fourth (signal) beam. There are a number of effects that can yield the desired refractive index modulation, such as saturable absorption, thermally induced refractive index changes, and the optical Kerr effect.[27] The time-dependent behavior of the PC signal is related to the development and persistence of the grating and therefore conveys information on the various relaxation mechanisms of the nonlinear medium.

In some of the previous studies on the third-order optical nonlinearity of C_{60} in different media,[7,8,14,16,18,25] evidence was presented of the existence of two components in the nonlinearity, one of them with a response on the picosecond time scale and the other with a decay time much longer than picoseconds. It was suggested[7,8,18,25] that the slow component could originate from a thermal grating created by the nonuniform heating of the medium by the interacting beams, but no further investigation was carried out on this component, and only Vijaya *et al.*[7] presented an estimation of the value of the third-order nonlinear susceptibility $\chi^{(3)}$ for C_{60} in toluene that is due to a thermal mechanism.

In a previous paper[29] we concentrated on the study of the long-lived component of the nonlinearity in solutions of C_{60} and C_{70} in toluene. The relevant aspects of the nonlinear process were investigated by an approach that had been demonstrated to be effective in nonlinear studies in other species,[30,31] and evidence was presented confirming that the long-lived component of the third-order optical nonlinearity was caused by a thermal grating. Values for the thermally induced third-order susceptibilities were estimated, and the effective thermalization at a given time was considered. In this paper we extend those studies to solutions of C_{60} in a number of solvents with different characteristic parameters. The existence is well-known of substantial electronic and vibrational interactions between solvent and C_{60} that result in varying solvatochromic shifts across the entire C_{60} spectrum, depending on the solvent used.[32−34] An investigation of the phase-conjugation properties of different C_{60}/solvent combinations could provide complementary information about these interactions. Two criteria were followed in selecting the solvents: (a) the solubility of C_{60} should be high enough to allow concentrations on the order 0.5 mM, and (b) the solvent should not absorb at the irradiation wavelength and give no appreciable PC signal, in our experimental conditions. Two aromatic (benzene and *p*-xylene) and two aliphatic (trichloroethylene and carbon tetrachloride) solvents complying with the above criteria were chosen.

The experiments were performed using nanosecond laser pulses at 365 nm, in the region of the orbitally allowed singlet−singlet transitions.[35] In each C_{60}/solvent system we investigated the effect on the response of the nonlinear medium of aspects such as read beam time delay, solute concentration, time delay between writing beams, and intensities of pump beams. Oscillatory acoustic modes generated by the nonuniform heating of

† FAX: +341 564 24 31. E-mail: acostela@igfr.csic.es.

⊗ Abstract published in *Advance ACS Abstracts,* June 1, 1997.

S1089-5647(97)00285-X CCC: $14.00

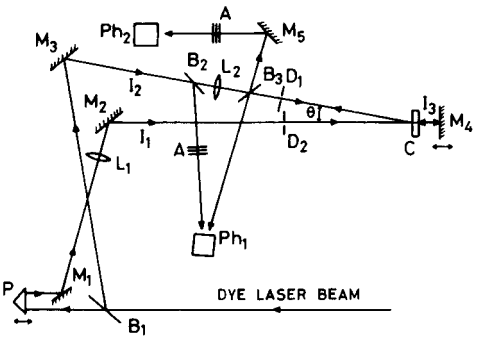

Figure 1. Schematic of experimental arrangement for DFWM using the retroreflection geometry: (A) attenuators; (B) beam splitters; (C) sample cell; (D) iris diaphragms; (L) lenses; (M) mirrors; (P) prism; (Ph) photodiodes; (I_1, I_3) pump beams; (I_2) probe beam; $\theta = 5°$.

the medium were detected, and the mechanism responsible for the slow component of the third-order nonlinearity was found to be thermal in all cases. Thermally induced third-order susceptibilities were estimated, and the influence of the solvent on the results obtained was analyzed.

Experimental Section

A schematic diagram of the experimental arrangement is shown in Figure 1. A standard retroreflection DFWM geometry was used.[36] All three input beams (probe, forward, and backward pump) were obtained from the ouput of a homemade XeCl-laser-pumped dye laser. This dye laser consisted of a Shoshan-Littman type[37,38] oscillator followed by two amplifier stages and used as the active medium a solution of DMQ (2-methyl-5-*tert*-butyl-*p*-quaterphenyl) in 1,4-dioxane. This system produced UV pulses at 365 nm of s-polarized radiation with energy up to 1.5 mJ/pulse. The pulse duration was ~4.5 ns fwhm with a spectral line width of <0.2 cm^{-1}. A quartz beam splitter (B_1) divided the dye laser ouput into a high-intensity (I_1) forward pump beam and a low-intensity (I_2) probe beam. The overlap in time of the two beams at the position of the nonlinear medium can be adjusted by varying the position of prism P in an optical delay line placed in the path of the forward pump beam. The counterpropagating pump beam (I_3) was obtained by retroreflecting I_1 in an aluminum plane mirror (M_4) positioned behind the 0.1-cm-long sample cell (C) containing the nonlinear medium. The position of this mirror can be varied so that different time delays between beams I_3 and I_1, I_2 can be introduced. The beams I_1 and I_2 were focused into the sample cell with 100 cm and 50 cm focal length quartz lenses, respectively, unless otherwise stated. The probe and pump beams crossed at an angle of 5° at the position of the cell. The phase-conjugate reflection of the probe wave was detected by using a beam splitter (B_3) and a fast rise time photodiode (Ph_1) (ITL TF1850). A beam splitter (B_2) directed a small fraction of the probe beam through appropriate attenuators toward the same photodiode Ph_1, allowing direct comparison of temporal shape and pulse duration between probe and phase-conjugate signals. Shot-to-shot energy fluctuations were registered by diverting another small fraction of the probe beam toward photodiode Ph_2 (EG&G SGD-100) via beam splitter B_3 and mirror M_5. The integrated output of Ph_2 was calibrated against a GenTec ED-100A pyroelectric energy meter, which was used to measure pulse energies. Typical energies of forward pump and probe beams at the position of the cell were 350 and 100 μJ, respectively. Phase-conjugate reflectivity was calibrated by using a mirror, of known reflectivity, positioned normal to the probe beam in the position of the sample. Iris diaphragms D_1 and D_2 inserted in the probe and pump beam paths helped to keep unwanted reflections from reaching photodiode Ph_1. The phase-conjugate nature of the signal was inferred from the disappearance of the signal when either of the two pump beams or the probe beam was blocked, demonstrating the optical *and* gate property predicted by DFWM theory,[28] as well as by the shortened pulse length (~2.5 ns fwhm) of the reflected beam. No actual aberration correction experiments were performed.

Solutions of C_{60} in benzene, carbon tetrachloride, *p*-xylene, and trichloroethylene were used as nonlinear media. Fullerenes were obtained by arc-vaporizing graphite under 350 mbars of helium in a reactor built following the directions of Scrivens and Tour.[39] Once the fullerene mixture is formed in the arc, it is extracted from the soot with toluene, placing the reactor in an ultrasonic bath. The nonsoluble material was separated from the extract by centrifugation at 6000 rpm and filtration in WCVP Millipore membranes with 0.1 μm pore size. The extract was then concentrated and dried using a Rotovap at ~80 °C and 0.01 mbar.

Separation of C_{60} from the obtained product was accomplished by column liquid chromatography on PGH graphite powder according to a method based on that of Spitsyna *et al.*[40] From the first fractions C_{60} was obtained with 99.5% purity. The analysis was carried out by high-perfomance liquid cromatography (HPLC) in a HPLC Kontron 325 chromatograph with a 432 detector and a 250 × 4 mm column filled with Spherisorb ODS2 (5 μm grain size), at a detector wavelength of 330 nm. The moving phase was 50:50 toluene/acetonitrile.

The characteristics and purity of the products and solvents used are as follows: graphite rods, 120 mm length and 6 mm diameter, from Le Carbone Lorraine, PT quality; DMQ (Exciton), laser grade; carbon disulfide (BDH), spectroscopic grade; carbon tetrachloride (Riedel de Haen), chromatographic grade; *p*-xylene (Panreac) and trichloroethylene (Panreac), PRS, 98%; 1,4-dioxane (Panreac), 99%; acetonitrile (Scharlau), HPLC grade, 99.85%; toluene (Romil Chemicals) and benzene (Aldrich), HPLC grade, 99.9%. The solvents were used as received.

Fullerene molecules in solution have been shown to degrade at high laser power densities by a photolysis mechanism, especially under irradiation of UV and visible light.[41] To ascertain that sample degradation is not affecting the DFWM results, UV−visible absorption spectra of the C_{60} solutions were taken before and after each experiment with a Cary 1E UV−visible spectrophotometer. The invariance of the spectra excluded any effect of photodegradation in our experimental conditions.

Results and Discussion

The concentration of C_{60} in each solvent was adjusted to optimize the phase-conjugate reflectivity. The concentrations producing the highest reflectivities were found to be 0.17, 0.44, 0.1, and 0.19 mM, for benzene, carbon tetrachloride, *p*-xylene, and trichloroethylene solvents, respectively. With these concentrations of C_{60} the transmission of the solutions in the 0.1-cm-long cell at 365 nm was ~50%.

All the experiments were performed with the counterpropagating pump beam I_3 arriving at the nonlinear medium with a time delay of at least 0.12 ns with respect to probe and forward pump beams. In these conditions there is no contribution to the observed PC signal from the short-lived component of the nonlinearity, which decays in less than 30 ps.[8] Contributions from the solvents represented at most 2% of the signal obtained when C_{60} was present. The phase-conjugate signal was very sensitive to the temporal overlap between probe and forward pump pulses, as seen in Figure 2 for solutions of C_{60} in *p*-xylene and carbon tetrachloride. Similar results were obtained with

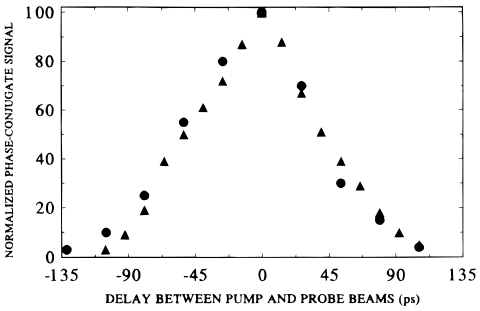

Figure 2. Normalized phase-conjugate signal as a function of the optical delay between probe and forward pump pulses for solutions of C_{60} in carbon tetrachloride (▲) and *p*-xylene (●).

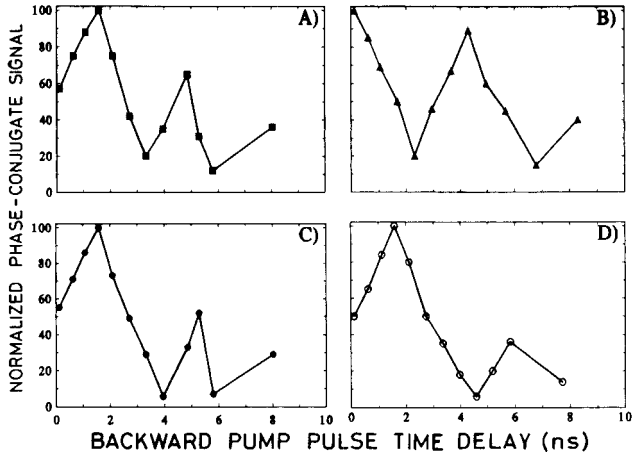

Figure 3. Normalized phase-conjugate signal as a function of the backward pump pulse time delay relative to the "write" beams for solutions of C_{60} in (A) benzene, (B) carbon tetrachloride, (C) *p*-xylene, and (D) trichloroethylene. The solid lines are guidelines for the eye.

the other samples. This is to be expected for a nonlinear mechanism characterized by a slow relaxation time:[42] as the hologram formed in the medium by the interference of the writing beams is effectively integrated over the duration of the laser pulse, the degree of mutual coherence of the interfering beams must be high if large PC reflectivities are to be observed. This condition implies that the difference in arrival times at the sample between the forward pump and probe pulses should be kept much smaller than the coherence time of the laser radiation.

There is a second grating in the medium, produced by the interference between the backward pump and probe beams. The results shown in Figure 2, indicating the importance of the interfering beams being precisely coherent, allow us to rule out any significant contribution of this second grating to the PC reflectivity in our experimental configuration, because of the time delay between beams I_3 and I_2.

In Figure 3 we present measurements of the phase-conjugate reflectivity as a function of the delay of the backward pump pulse ("read" pulse) relative to the "write: beams for the different media studied in the present work. In these experiments, the forward pump beam was not focused into the cell in order to facilitate the control of the backward pump beam intensity. Clearly seen in Figure 3 is an oscillatory behavior of the long-lived component of the DFWM signal as a function of the backward pump time delay. This modulation of the PC reflectivity, which was also observed in solutions of C_{60} in toluene,[29] could be explained in the same way, namely, by the excitation of coherent acoustic waves in the media throughout a nonuniform heating mechanism.[43−46] Absorption at 365 nm promotes electrons to an excited singlet state S_n ($n > 1$).[35]

TABLE 1: Solvents' Constants Used in Numerical Computations

quantity[a]	*p*-xylene	benzene	carbon tetrachloride	trichloro-ethylene
n (20 °C)[b]	1.4958	1.5011	1.4664	1.4706
$(dn/dT)_p$ (K^{-1})[c]	-5.2×10^{-4}	-5.1×10^{-4}	-5.7×10^{-4}	-5.2×10^{-4}
ρ (g/cm^3) (20 °C)[b]	0.861	0.8787	1.5942	1.4405
C_p [erg/(gK)][d]	1.73×10^7	1.745×10^7	0.905×10^7	1.15×10^7
C_v [erg/(gK)][d]	1.43×10^7	1.50×10^7	0.744×10^7	0.99×10^7
η (poise)[b]	0.603×10^{-2}	0.604×10^{-2}	0.908×10^{-2}	0.545×10^{-2}
κ [erg/(s cm K)][b]	1.57×10^4	1.577×10^4	1.03×10^4	1.16×10^4
v_s (cm/s)[b]	1.334×10^5	1.295×10^3	0.926×10^5	1.049×10^5

[a] n refractive index; $(dn/dT)_p$ derivative of the index of refraction with respect to temperature at constant pressure; ρ density; C_p specific heat at constant pressure; C_v specific heat at constant volume; η viscosity; κ thermal conductivity; v speed of sound. [b] Reference 50. [c] Reference 51. [d] Reference 52.

TABLE 2: Grating and Acoustic Parameters[a] for the Different Solvents

solvent	Λ (mm)	τ_{ac} (ns)	τ_R (μs)	ω_B^{-1} (ns)	$2/\Gamma_B$ (μs)
p-xylene	4.44	3.3	4.7	0.53	1.4
benzene	4.41	3.4	4.8	0.54	1.4
carbon tetrachloride	4.52	4.9	7.2	0.78	1.8
trichloroethylene	4.52	4.3	7.4	0.68	2.7

[a] Λ grating spacing; τ_{ac} acoustic period; τ_R Rayleigh lifetime; ω_B Brillouin frequency; Γ_B Brillouin line width.

Nonradiative relaxation to S_1 and subsequent relaxation to T_1 by rapid and efficient intersystem crossing[47,48] results in deposition of heat in the medium into the peaks of the interference pattern formed by I_1 and I_2, giving rise to a periodic temperature distribution, or thermal grating, in the medium. The nonuniform heating of the medium results in the production of sound waves that propagate across it, giving rise to time-dependent spatially periodic changes in the material's density and, therefore, in its refractive index. In this way, the thermal grating is modulated at a frequency v_s/Λ, where v_s is the speed of sound propagation in the medium and Λ is the grating spacing.

From the grating equation,[49] Λ can be calculated to be

$$\Lambda = \frac{\lambda_0}{2n \sin(\theta/2)} \quad (1)$$

where λ_0 is the wavelength in vacuum of the interfering beams, n is the refractive index of the medium, and θ is the angle in the medium between the interfering beams. Under our experimental conditions, and using the appropriate values for n (Table 1), the values tabulated in Table 2 are obtained for Λ. Combining these values with the speed of sound propagation in the different media (Table 1), the acoustic periods tabulated in Table 2 are predicted, which are in qualitative agreement with the periods of the modulations apparent in Figure 3.

If the dominant contribution to the generation of the long-lived component of the nonlinearity is due to a thermal grating, the theoretical treatment of Hoffman[53] can be applied. In this theory, a coupled hydrodynamic−electromagnetic formalism is used to describe the formation of thermal gratings in absorbing liquid solutions, and a relatively simple analytical expression is derived for the reflectivity R, or ratio of conjugate signal and probe beam intensities:

$$R \simeq f^2 Q^2 \exp(-\alpha L/\cos\theta)[(1 - \exp(-\alpha L)]^2 I_1 I_3 G(t_D) \quad (2)$$

where I_1 (I_3) represents the intensity of the forward (backward)

pump beam, α denotes the absorption coefficient, L is the length of the nonlinear medium, and Q is a constant given by

$$Q = -\frac{2\pi(\mathrm{d}n/\mathrm{d}T)_p}{\lambda_0 \rho C_p} \tag{3}$$

where $(\mathrm{d}n/\mathrm{d}T)_p$, ρ, and C_p are the derivative of the index of refraction with respect to temperature at constant pressure, the density, and the specific heat of the solvent at constant pressure, respectively.

The factor $G(t_D)$, where t_D represents the time delay of the backward pump pulse relative to the "write" beams, contains details of the thermal grating evolution, and f is a phenomenological factor that can be considered a material's figure of merit effectively characterizing the thermalization yield for a given time delay.

Approximate expressions for $G(t_D)$ can be obtained under suitable conditions. For small backward pump time delays ($t_D < t_p - t_p'$, where t_p and t_p' are the probe and conjugate beam pulse lengths, respectively), $G(t_D)$ can be written, in first-order approximation, as[53]

$$G(t_D) \approx \frac{(t_p')^2}{3\tau^2\Gamma_u^2}\left[1 + \frac{3t_D(t_D + t_p')}{(t_p')^2}\right] \tag{4}$$

where τ is the effective solute thermalization time and $1/\Gamma_u$ represents the thermalization time due to noninstantaneous and nonlocal solute−solvent energy transfer. Both parameters are related to the diffusion coefficient D of the solute molecules in the solvent:

$$\tau\Gamma_u = 1 + \tau D q^2 \tag{5}$$

where $q = 2k \sin \theta/2$ is the grating wave vector with $k = 2\pi n/\lambda_0$.

The expression (4) is obtained under the assumptions

$$\omega_B^{-1} < t_p, t_p' \ll \tau_R, 2/\Gamma_B \tag{6}$$

$$\tau, \Gamma_u^{-1} \ll \tau_R, 2/\Gamma_B \tag{7}$$

where $\omega_B = v_s q$ is the Brillouin frequency in the solvent, and Γ_B denotes the full Brillouin line width defined through the relation

$$\Gamma_B = \Gamma_B' + \frac{(\gamma - 1)}{\tau_R} \tag{8}$$

where $\Gamma_B' = \eta q^2/\rho_0$ is the viscous contribution to the Brillouin line width, with η being the effective viscosity, and $\gamma = C_p/C_v$ is the ratio of specific heats at constant pressure and constant volume, respectively. Finally, τ_R is the Rayleigh lifetime, which governs the decay time of the thermal grating, and is given by[54]

$$\tau_R = \frac{\rho_0 C_p \Lambda^2}{4\pi^2 \kappa} \tag{9}$$

where κ is the thermal conductivity of the solvent and the other parameters have been defined previously.

By using the appropriate values for the solvents' constants (Table 1) and gratings' spacings (Table 2), the values of τ_R, ω_B^{-1}, and $2/\Gamma_B$ listed in Table 2 are obtained for the different solvents. It is inmediately seen that condition (6) is fulfilled in the present experiments. Condition (7) needs further consideration, as neither the effective thermalization time τ nor the energy transfer time Γ_u^{-1} are known with sufficient precision. Nevertheless, it is still possible to obtain an order of magnitude estimation of these parameters by examining the conditions of development of the thermal grating and using eq 5. In our case, the thermalization can be assumed to be due primarily to the relaxation processes of the excited fullerene molecules, first to the equilibrium singlet state S_1 and then to the triplet state T_1. The first process takes place in picoseconds and the second one in ~1 ns,[48] so that τ should be on the nanosecond time scale. On the other hand, a rough estimation of the diffusion coefficient D of C_{60} in the different solvents can be obtained from the diffusion theory in liquid solutions, which predicts[55]

$$D = \frac{kT}{6\pi\eta\alpha} \tag{10}$$

where k is the Boltzmann's constant, T is the absolute temperature, and α is the radius of the particle diffusing in the solvent of viscosity η. The diameter of the C_{60} molecule has been determined to be about 7.1 Å.[56] Using this value together with the viscosoties listed in Table 1 for the different solvents, eq 10 gives values of D at room temperature ranging from 3.4×10^{-6} cm^2/s (carbon tetrachloride) to 5.6×10^{-6} cm^2/s (trichloroethylene). Thus, even allowing for values of D several orders of magnitude higher than those calculated from the diffusion theory, $\tau D q^2 \ll 1$ is obtained. Hence, from eq 5 $\tau\Gamma_u \approx 1$, $\Gamma_u^{-1} \approx \tau$, and condition (7) is fulfilled. In addition, eq 4 can be simplified to

$$G(t_D) \approx \frac{(t_p')^2}{3}\left[1 + \frac{3t_D(t_D + t_p')}{(t_p')^2}\right] \tag{11}$$

Figure 4 presents the dependence of the PC reflectivity on the concentration of C_{60} in the different solvents for pump and probe beam intensities of ~14 and ~2.5 MW/cm^2, respectively, and a backward pump pulse time delay of 0.12 ns. In Figure 5 the PC reflectivity, at the same time delay of 0.12 ns, is represented as a function of the pump beams' intensity product $I_1 I_3$ for the optimum concentrations of C_{60} as determined from Figure 4. No signs of saturation are seen in the results presented in Figure 5, as is to be expected in the low-reflectivity regime.

The solid lines in Figure 4 were obtained by applying eq 2 with the expression (11) for $G(t_D)$, the appropriate constants for the different solvents (Table 1), and with f as a free parameter. The values of f that best fitted the experimental points for each C_{60}−solvent combination are listed in the first column of Table 3. These values of f are the same as those predicted from the slope of the best linear fit to the experimental points in Figure 5. It is observed in Table 3 that the fitted thermalization yields only differ by ~6%. These differences, albeit small, are significant: changing the values of f by ±5% results in strong deviations from the experimental behavior, with the theoretical curves in Figure 4 missing the experimental points by ~25%.

An alternative theoretical approach based on a population grating formalism[57] was also tried to analyze our experimental results. Using the expression for the PC reflectivity predicted by this approach, we were not able to reproduce the above experimental results. This outcome, together with the good agreement with experiment yielded by the thermal grating theory and the support for the existence of a heating mechanism provided by the modulation of the PC reflectivity as a function of t_D (Figure 3), strongly suggests that in our experimental conditions thermal effects, rather than excited-state population, are the main factors that are responsible for the long-lived

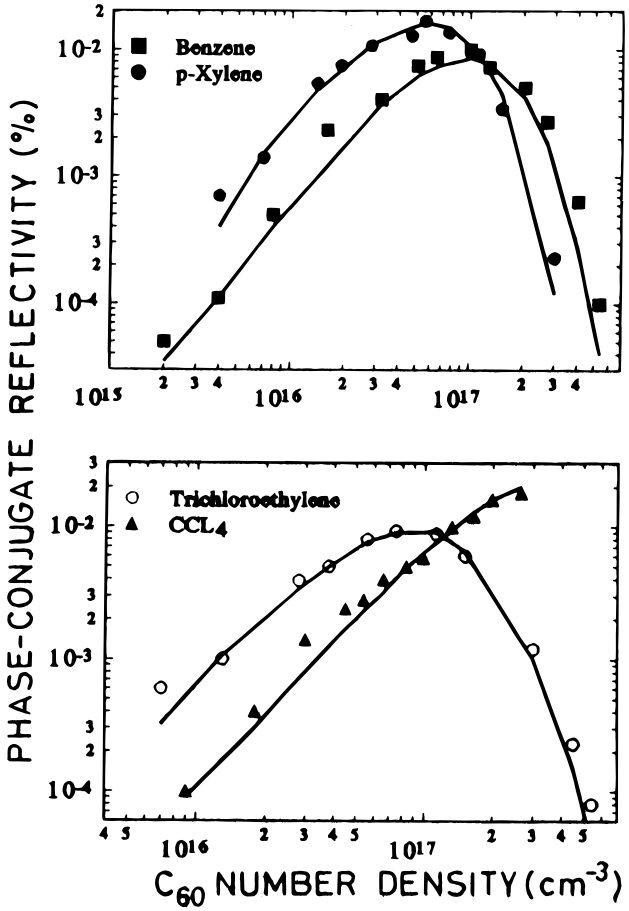

Figure 4. Measured phase-conjugate reflectivity as a function of the concentration of C_{60} in the different solvents. $I_1 \approx 14$ MW/cm^2; $I_2 \approx 2.5$ MW/cm^2; $t_D = 0.12$ ns. The solid lines are a plot of eq 2 with the values of f listed in the first column of Table 3.

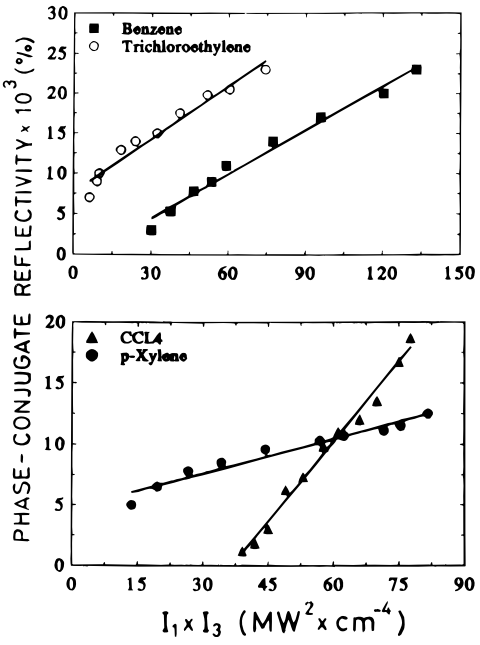

Figure 5. Measured phase-conjugate reflectivity as a function of the product of the intensities of the pump beams for the different C_{60} solutions. $I_2 \approx 2.5$ MW/cm^2; $t_D = 0.12$ ns. The solid lines represent the best linear fit to the experimental points.

component of the nonlinearity. Similar conclusions were obtained by Liu *et al.*[18] from DFWM experiments performed on solutions of C_{60} in toluene with 20 ps pulses at 532 nm, which showed that scattering due to excited-state populations played a minor role in the generated PC signal.

TABLE 3: Estimated and Derived Parameters for Solutions of C_{60} in the Different Solvents and Values for the Solvents' Polarizability

solvent	f (t_D = 0.12 ns)[a]	f (t_D, ns)[b]	$\lvert\chi^{(3)}\rvert$[c] (m^2 V^{-2})	$(n^2-1)/(2n^2+1)$[d]
p-xylene	0.92	0.16 (5.3)	$1.8 \times 10{-}18$	0.226
benzene	0.90	0.19 (2.7)	$1.8 \times 10{-}18$	0.228
carbon tetrachloride	0.96	0.23 (3.7)	$1.9 \times 10{-}18$	0.217
trichloroethylene	0.95	0.28 (2.7)	$1.7 \times 10{-}18$	0.218

[a] Values of f obtained from eq 2 for backward pump pulse time delay of 0.12 ns. [b] Values of f obtained from eq 2 for the backward pump pulse time delays indicated in parentheses. [c] $\chi^{(3)}$: thermally induced nonlinear susceptibility. [d] Solvent's polarizability parameter; n, refractive index.

The above values of the parameter f were determined at backward pump time delays about 10 times shorter than the singlet to triplet transfer time.[48] Thus, the main contribution to the formation of the thermal grating should proceed from the energy released in the fast processes taking place in the singlet manifold after the absorption of the exciting radiation. As seen in Table 3, there is a difference in the values of f depending on the solvent being aromatic or aliphatic. In aromatic solvents, the close-lying nature of C_{60}-allowed transitions to the electronic transitions of the solvents suggests that there will be some mixing of solute and solvent excited states.[32] It is expected that the solvent−solute interaction occurs through a π-stacking arrangement, which could be an important factor in the stabilization of C_{60} and C_{60}* and suggests that the C_{60} surface is electronically very sensitive to its environment.[32,34] In fact, the largest bathochromic shift across the entire spectrum of C_{60} is induced by aromatic solvents, where the diffuse electron density (*i.e.* polarizability) is best able to stabilize the electronic transition.[32] In the present study a significant correlation was found between f values and solvents' polarizability parameter, $(n^2-1)/(2n^2+1)$ (Table 3), which seems to indicate that the parameter f, which comprises an average of different relaxation processes, depends on the solvent/C_{60} interaction processes. Thus, the differences in the values of f apparent in Table 3 are reflecting differences in interaction between C_{60} molecules and the different solvents.

An estimation of the thermally induced nonlinear third-order susceptibility can be obtained from the expression[57]

$$\chi^{(3)} = \left(\frac{dn}{dT}\right)\frac{4n^2 c\epsilon_0 \alpha t_p f}{3\rho C_p} \qquad (12)$$

that is valid when the mechanism principally responsible for the nonlinearity in the medium is that of thermally induced refractive index changes. In eq 12 ϵ_0 is the dielectric permittivity of vacuum, and the other parameters have been defined previously. Using the above expression with the appropriate values for the different parameters, the values of $|\chi^{(3)}|$ listed in Table 3 are obtained. These values are within the same order of magnitude as those previously estimated for C_{60} in toluene due to a thermal mechanism.[7,29]

Information about the kinetics of the thermalization processes in the different media can be obtained from the values of the parameter f at different read beam delays. As an example, Figure 6 shows the PC reflectivity as a function of I_1I_3 for backward pump time delays in the range 2.7−5.3 ns. A good linearity is observed in all cases, and from the slopes of the straight lines fitting the experimental data and the use of eq 2 the corresponding values of f can be obtained. It should be

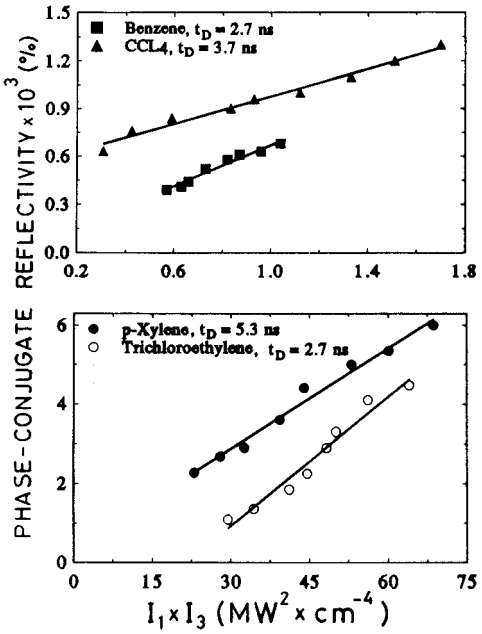

Figure 6. Measured phase-conjugate reflectivity as a function of the product of the intensities of the pump beams for the different C_{60} solutions with read beam time delays in the range 2.7−5.3 ns. $I_2 \approx 2.5$ MW/cm^2. The solid lines represent the best linear fit to the experimental points.

noticed that in this case the expression (11) for $G(t_D)$ is no longer valid as condition $t_D < t_p - t_p'$ is not satisfied. In the region $t_D \geq t_p$, the expression (4) for $G(t_D)$ should be replaced by[53]

$$G(t_D) \approx \frac{t_p^2}{\tau^2 \Gamma_u^2} \exp\left(-\frac{2t_D}{\tau_R}\right) \qquad (13)$$

As in our experimental conditions $\tau\Gamma_u$ can be approximated by unity (see discussion before eq 11), the above expression can be written

$$G(t_D) \approx t_p^2 \exp\left(-\frac{2t_D}{\tau_R}\right) \qquad (14)$$

For the intermediate-delay region $t_p - t_p' < t_D < t_p$, an extrapolation between the two extremes can be used.

Using once more the values listed in Table 1 for the solvents' constants, the values of f listed in the second column of Table 3 are predicted. These values are smaller than those obtained when $t_D = 0.12$ ns, which is to be expected because once the transfer of energy to the medium is complete and the thermal grating is fully developed, thermal diffusion begins to erode the grating, and the value of f, which represents the effective thermalization at a given time, should decrease.

Summary and Conclusions

In the present work we have carried out an investigation on the phase-conjugate properties of solutions of buckminsterfullerene C_{60} in a number of solvents, both aromatic and aliphatic. The technique used was degenerate four-wave mixing in the nanosecond time scale regime, and we concentrate on the study of the long-lived component of the third-order optical nonlinearity. The effects on the process efficiency of variables such as time delay between writing beams, solute concentration, intensities of the pump beams, and read beam time delay were evaluated. The results obtained were found to be consistent with a thermal mechanism for the long-lived component of the nonlinearity. In particular, evidence was obtained of the excitation of coherent acoustic waves in the medium throughout a nonuniform heating mechanism.

The experimental results were quantitatively analyzed using established theory,[53] and a significant correlation between effective thermalization yield and solvents' polarizability parameter was found, reflecting differences in solvent/C_{60} interaction processes depending on the solvents' characteristics. Order of magnitude estimations were obtained for the thermally induced nonlinear third-order susceptibility, and it was shown that probing the nonlinearity at different read beam time delays could be a useful technique to get information about the kinetics of the thermalization processes in the diferent media.

Acknowledgment. This work was supported by Project No. MAT94-0757 of the Spanish CICYT.

References and Notes

(1) Kroto, H. W.; Allaf, A. W.; Balm, S. P. *Chem. Rev.* **1991**, *91*, 1213.
(2) Wang, Y.; Cheng, L. *J. Phys. Chem.* **1992**, *96*, 1530.
(3) Blau, W. J.; Byrne, H. J.; Cardin, D. J.; Dennis, T. J.; Hare, J. P.; Kroto, H. W.; Taylor, R.; Walton, D. R. M. *Phys. Rev. Lett.* **1991**, *67*, 1423.
(4) Kafafi, Z. H.; Lindle, J. R.; Pong, R. G. S.; Bartoli, F. J.; Lingg, L. J.; Milliken, J. *Chem. Phys. Lett.* **1992**, *188*, 492.
(5) Gong, Q.; Sun, Y.; Xia, Z.; Zou, Y. H.; Gu, Z.; Zhou, X.; Qiang, D. *J. Appl. Phys.* **1992**, *71*, 3025.
(6) Yang, S.; Gong, Q.; Xia, Z.; Zou, Y. H.; Wu, Y. Q.; Qiang, D.; Sun, Y. L.; Gu, Z. N. *Appl. Phys. B* **1992**, *55*, 51.
(7) Vijaya, R.; Murti, Y. V. G. S.; Sundararajan, G.; Mathews. C. K.; Vasudeva Rao, P. R. *Opt. Commun.* **1992**, *94*, 353.
(8) Zhang, Z.; Wang, D.; Ye, P.; Li, Y.; Wu, P.; Zhu, D. *Opt. Lett.* **1992**, *17*, 973.
(9) Talapatra, G. B.; Manickam, N.; Samoc, M.; Orczyk, M. E.; Karna, S. P.; Prasad, P. N. *J. Phys. Chem.* **1992**, *96*, 5206.
(10) Rosker, M. J.; Marcy, H. O.; Chang, T. Y.; Khoury, J. T.; Hansen, K.; Whetten, R. L. *Chem. Phys. Lett.* **1992**, *196*, 427.
(11) Meth, J. S.; Vanherzeele, H.; Wang, Y. *Chem. Phys. Lett.* **1992**, *197*, 26.
(12) Henari, F.; Callagham, J.; Stiel, H.; Blau, W.; Cardin, D. J. *Chem. Phys. Lett.* **1992**, *199*, 144.
(13) Neher, D.; Stegeman, G. I.; Tinker, F. A.; Peyghambarian, N. *Opt. Lett.* **1992**, *17*, 1491.
(14) Aranda, F. J.; Rao, D. V. G. L. N.; Roach, J. F.; Tayebati, P. *J. Appl. Phys.* **1993**, *73*, 7949.
(15) Tang, N.; Partanen, J. P.; Hellwarth, R. W.; Knize, R. J. *Phys. Rev. B* **1993**, *48*, 8404.
(16) Lindle, J. R.; Pong, R. G. S.; Bartoli, F. J.; Kafafi, Z. H. *Phys. Rev. B* **1993**, *48*, 9447.
(17) Ji, W.; Tang, S. H.; Xu, G. Q.; Chan, H. S. O.; Ng, S. C.; Ng, W. W. *J. Appl. Phys.* **1993**, *74*, 3669.
(18) Liu, H.; Taheri, B.; Jia, W. *Phys. Rev. B* **1994**, *49*, 10166.
(19) Kajzar, F.; Taliani, C.; Danieli, R.; Rossini, S.; Zamboni, R. *Chem. Phys. Lett.* **1994**, *217*, 418.
(20) Yang, L.; Dorsinville, R.; Alfano, R. *Chem. Phys. Lett.* **1994**, *226*, 605; *Chem. Phys. Lett.* **1995**, *232*, 186 (erratum).
(21) Couris, S.; Koudoumas, E.; Ruth, A. A.; Leach, S. *J. Phys. B: At. Mol. Opt. Phys.* **1995**, *28*, 4537.
(22) Hess, B. C.; Bowersox, D. V.; Mardirosian, S. H.; Unterberger, S. H. *Chem. Phys. Lett.* **1996**, *248*, 141.
(23) Geng, L.; Wright, J. C. *Chem. Phys. Lett.* **1996**, *249*, 105.
(24) Taheri, B.; Liu, H.; Jassemnejad, B.; Appling, D.; Powell, R. C.; Song, J. J. *Appl. Phys. Lett.* **1996**, *68*, 1317.
(25) Liu, H.; Taheri, B.; Jia, W.; Lin, F.; Mao, S. *Appl. Phys. Lett.* **1996**, *68*, 1570.
(26) Couris, S.; Koudoumas, E.; Dong, F.; Leach, S. *J. Phys. B: At. Mol. Opt. Phys.* **1996**, *29*, 5033.
(27) Fisher, R. A., Ed. *Optical Phase Conjugation*; Academic Press: New York, 1983.
(28) Yariv, A. *IEEE J. Quantum Electron.* **1978**, *QE-14*, 650.
(29) Costela, A.; García-Moreno, I.; Saiz, J. L. *J. Opt. Soc. Am. B* **1997**, *14*, 615.
(30) Costela, A.; Figuera, J. M.; Florido, F. *Opt. Commun.* **1993**, *100*, 536.
(31) Costela, A.; García-Moreno, I. *Chem. Phys.* **1996**, *206*, 383.
(32) Gallagher, S. H.; Armstrong, R. S.; Lay, P. A.; Reed, C. A. *J. Phys. Chem.* **1995**, *99*, 5817.
(33) Renge, I. *J. Phys. Chem.* **1995**, *99*, 15955.

(34) Gallagher, S. H.; Armstrong, R. S.; Lay, P. A.; Reed, C. A. *Chem. Phys. Lett.* **1996**, *248*, 353.
(35) Leach, S.; Vervloet, M.; Desprès, A.; Bréheret, E.; Hare, J. P.; Dennis, T. J.; Kroto, H. W.; Taylor, R.; Walton, D. R. M. *Chem. Phys.* **1992**, *160*, 451.
(36) Pepper, D. M. *Opt. Eng.* **1982**, *21*, 156.
(37) Shoshan, I.; Danon, N. M.; Oppenheim, U. P. *J. Appl. Phys.* **1977**, *48*, 4495.
(38) Littman, M. G.; Metcalf, H. J. *Appl. Opt.* **1978**, *17*, 2224.
(39) Scrivens, W. A.; Tour, J. M. *J. Org. Chem.* **1992**, *57*, 6932.
(40) Spitsyna, N. G.; Buravov, L. I.; Lobach, A. S. *J. Anal. Chem.* **1995**, *50*, 613.
(41) Juha, L.; Hamplová, V.; Kubát, P.; Koudoumas, E.; Couris, S. *Chem. Phys. Lett.* **1994**, *231*, 314.
(42) Caro, R. G.; Gower, M. C. *Appl. Phys. Lett.* **1981**, *39*, 855.
(43) Salcedo, J. R.; Siegmann, A. E. *IEEE J. Quantum Electron.* **1979**, *QE-15*, 250.
(44) Nelson, K. A.; Lutz, D. R.; Fayer, M. D.; Madison, L. *Phys. Rev. B* **1981**, *24*, 3261.
(45) Nelson, K. A.; Dwayne Miller, R. J.; Lutz, D. R.; Fayer, M. D. *J. Appl. Phys.* **1981**, *53*, 1144.
(46) Desai, R. C.; Levenson, M. D.; Barker, J. A. *Phys. Rev. A* **1983**, *27*, 1968.
(47) Palit, D. K.; Sapre, A. V.; Mittal, J. P.; Rao, C. N. R. *Chem. Phys. Lett.* **1992**, *195*, 1.
(48) Li, C.; Zhang, L.; Wang, R.; Song, Y.; Wang, Y. *J. Opt. Soc. Am. B* **1994**, *11*, 1356.
(49) Born, M.; Wolf, E. *Principles of Optics*, 5th ed.; Pergamon: Oxford, 1975; p 403.
(50) Weast, R. C., Ed. *Handbook of Chemistry and Physics*, 46th ed.; The Chemical Rubber Co.: Cleveland, 1965.
(51) Ruck, M. In *Landolt-Börnstein, Zahlenwerte und Funktionen aus Physik, Chemie, Astronomie, Gephysik, und Technik, II Band, Optische Konstanten*; Hellwege, K. H., Hellwege, A. M., Eds.; Springer: Berlin, 1962; Vol. 8, pp 573−636.
(52) Auer, A. In *Landolt-Börnstein, Zahlenwerte und Funktionen aus Physik, Chemie, Astronomie, Gephysik, und Technik, II Band, Kalorische Zustandsgrössen*; Schäfer, K., Lax, E., Eds.; Springer: Berlin, 1961; Vol. 4, pp 267−298.
(53) Hoffman, H. J. *IEEE J. Quantum Electron.* **1986**, *QE-22*, 552.
(54) Eichler, H.; Enterlein, G.; Glozbach, P.; Munschau, J.; Stahl, H. *Appl. Opt.* **1972**, *11*, 372.
(55) Jost, W. *Diffusion*; Academic Press: New York, 1990; p 462.
(56) Liu, S.; Lu, Y.; Kappes, M. M.; Ibers, J. A. *Science* **1991**, *254*, 408.
(57) Caro, R. G.; Gower, M. C. *IEEE J. Quantum Electron.* **1982**, *QE-18*, 1376.